



## Capacity of extracellular globins to reduce liver fibrosis via scavenging reactive oxygen species and promoting MMP-1 secretion

Vu Ngoc Hieu<sup>a,1</sup>, Le Thi Thanh Thuy<sup>a,1</sup>, Hoang Hai<sup>a</sup>, Ninh Quoc Dat<sup>b</sup>, Dinh Viet Hoang<sup>a,c</sup>, Ngo Vinh Hanh<sup>a</sup>, Dong Minh Phuong<sup>a</sup>, Truong Huu Hoang<sup>a</sup>, Hitomi Sawai<sup>d</sup>, Yoshitsugu Shiro<sup>d</sup>, Misako Sato-Matsubara<sup>a</sup>, Daisuke Oikawa<sup>e</sup>, Fuminori Tokunaga<sup>e</sup>, Katsutoshi Yoshizato<sup>f,g</sup>, Norifumi Kawada<sup>a,\*</sup>

<sup>a</sup> Department of Hepatology, Graduate School of Medicine, Osaka City University, Osaka, Japan

<sup>b</sup> Department of Pediatrics, Hanoi Medical University, Hanoi, Viet Nam

<sup>c</sup> Cho Ray Hospital, Ho Chi Minh City, Viet Nam

<sup>d</sup> Graduate School of Life Science, University of Hyogo, Hyogo, Japan

<sup>e</sup> Department of Pathobiochemistry, Graduate School of Medicine, Osaka City University, Osaka, Japan

<sup>f</sup> Academic Advisor's Office, PhoenixBio Co. Ltd., Hiroshima, Japan

<sup>g</sup> Endowed Laboratory of Synthetic Biology, Graduate School of Medicine, Osaka City University, Osaka, Japan

### ARTICLE INFO

#### Keywords:

Globin  
Anti-fibrotic therapy  
HSCs  
ROS  
Endocytosis

### ABSTRACT

**Background & aims:** Hepatic stellate cells (HSCs) are the primary cell type in liver fibrosis, a significant global health care burden. Cytoglobin (CYGB), a globin family member expressed in HSCs, inhibits HSC activation and reduces collagen production. We studied the antifibrotic properties of globin family members hemoglobin (HB), myoglobin (MB), and neuroglobin (NGB) in comparison with CYGB.

**Approach & results:** We characterized the biological activities of globins in cultured human HSCs (HHStCs) and their effects on carbon tetrachloride (CCl<sub>4</sub>)-induced cirrhosis in mice. All globins demonstrated greater antioxidant capacity than glutathione in cell-free systems. Cellular fractionation revealed endocytosis of extracellular MB, NGB, and CYGB, but not HB; endocytosed globins localized to intracellular membranous, cytoplasmic, and cytoskeletal fractions. MB, NGB, and CYGB, but not HB, scavenged reactive oxygen species generated spontaneously or stimulated by H<sub>2</sub>O<sub>2</sub> or transforming growth factor β1 in HHStCs and reduced collagen 1A1 production via suppressing COL1A1 promoter activity. Disulfide bond-mutant NGB displayed decreased heme and superoxide scavenging activity and reduced collagen inhibitory capacity. RNA sequencing of MB- and NGB-treated HHStCs revealed downregulation of extracellular matrix-encoding and fibrosis-related genes and HSC deactivation markers. Upregulation of matrix metalloproteinase (MMP)-1 was observed following MB and NGB treatment, and MMP-1 knockdown partially reversed globin-mediated effects on secreted collagen. Importantly, administration of MB, NGB, and CYGB suppressed CCl<sub>4</sub>-induced mouse liver fibrosis.

**Conclusions:** These findings revealed unexpected roles for MB and NGB in deactivating HSCs and inhibiting liver fibrosis development, suggesting that globin therapy may represent a new strategy for combating fibrotic liver disease.

## 1. Introduction

Liver fibrosis refers to the accumulation of extracellular matrix

\* Corresponding author. Department of Hepatology, Graduate School of Medicine, Osaka City University, 1-4-3 Asahimachi, Abeno, Osaka, 545-8585, Japan.

E-mail addresses: [hieu.hmu@gmail.com](mailto:hieu.hmu@gmail.com) (V.N. Hieu), [thuyt@med.osaka-cu.ac.jp](mailto:thuyt@med.osaka-cu.ac.jp) (L.T.T. Thuy), [hhai@med.osaka-cu.ac.jp](mailto:hhai@med.osaka-cu.ac.jp) (H. Hai), [dr.ninhquocdat@gmail.com](mailto:dr.ninhquocdat@gmail.com) (N.Q. Dat), [viethoanghmu@gmail.com](mailto:viethoanghmu@gmail.com) (D.V. Hoang), [ngovinhhanh@gmail.com](mailto:ngovinhhanh@gmail.com) (N.V. Hanh), [dongminhphuong15@gmail.com](mailto:dongminhphuong15@gmail.com) (D.M. Phuong), [dr.hoangbv108@gmail.com](mailto:dr.hoangbv108@gmail.com) (T.H. Hoang), [sawai@sci.u-hyogo.ac.jp](mailto:sawai@sci.u-hyogo.ac.jp) (H. Sawai), [yshiro@sci.u-hyogo.ac.jp](mailto:yshiro@sci.u-hyogo.ac.jp) (Y. Shiro), [m2076883@med.osaka-cu.ac.jp](mailto:m2076883@med.osaka-cu.ac.jp) (M. Sato-Matsubara), [oikawa.daisuke@med.osaka-cu.ac.jp](mailto:oikawa.daisuke@med.osaka-cu.ac.jp) (D. Oikawa), [ftokunaga@med.osaka-cu.ac.jp](mailto:ftokunaga@med.osaka-cu.ac.jp) (F. Tokunaga), [katsutoshi.yoshizato@phoenixbio.co.jp](mailto:katsutoshi.yoshizato@phoenixbio.co.jp) (K. Yoshizato), [kawadanori@med.osaka-cu.ac.jp](mailto:kawadanori@med.osaka-cu.ac.jp) (N. Kawada).

<sup>1</sup> These authors shared co-first authorship.

<https://doi.org/10.1016/j.redox.2022.102286>

Received 3 February 2022; Received in revised form 5 March 2022; Accepted 11 March 2022

Available online 19 March 2022

2213-2317/© 2022 Published by Elsevier B.V. This is an open access article under the CC BY-NC-ND license (<http://creativecommons.org/licenses/by-nc-nd/4.0/>).

**List of abbreviations**

|              |  |                  |  |
|--------------|--|------------------|--|
| $\alpha$ SMA | $\alpha$ -smooth muscle actin            | IF               | immunofluorescence                               |
| AST          | aspartate aminotransferase               | IFN              | interferon                                       |
| ALT          | alanine aminotransferase                 | LDH              | lactate dehydrogenase                            |
| BW           | body weight                              | $O_2^{\bullet-}$ | superoxide anion radical                         |
| COL1A1       | collagen type I A1                       | MB               | myoglobin  |
| CYGB         | cytoglobin                               | MMP-1            | matrix metalloproteinase-1                       |
| CPZ          | chlorpromazine                           | NGB              | neuroglobin                                      |
| DCFDA        | 2',7'-dichlorofluorescein diacetate      | $OH^{\bullet}$   | hydroxyl radical                                 |
| GAPDH        | glyceraldehyde-3-phosphate dehydrogenase | qRT-PCR          | quantitative real-time polymerase chain reaction |
| $H_2O_2$     | hydrogen peroxide                        | sd               | standard deviation                               |
| HB           | hemoglobin                               | SiR-FG           | sirius red and fast green                        |
| H&E          | hematoxylin and eosin                    | STAT             | signal transducer and activator of transcription |
| HHSteCs      | human hepatic stellate cells             | rh               | recombinant human                                |
| HSCs         | hepatic stellate cells                   | RNA-seq          | RNA-sequencing                                   |
| 4-HNE        | 4-hydroxy-2'-nonenal                     | ROS              | reactive oxygen species                          |
| HX-XO        | hypoxanthine-xanthine oxidase            | TAC              | total antioxidant capacity                       |
| IHC          | immunohistochemistry                     | TGF- $\beta$ 1   | transforming growth factor-beta 1                |
|              |  | WT               | wild-type  |

(ECM) proteins due to chronic liver injury of any etiology. Because sustained fibrosis leads to the development of end-stage cirrhosis and generates a microenvironment favorable to the development of primary liver cancer [1], early-stage treatment of liver fibrosis is essential. To date, although some antifibrotic agents have reached clinical trials, effective therapy for fibrosis and cirrhosis in clinical practice remains an unmet medical need [2].

Hepatic stellate cells (HSCs) are resident cells in the hepatic parenchyma and play an important role in the pathophysiology of liver fibrosis [3]. During chronic liver disease, several factors stimulate HSC activation, including proinflammatory cytokines secreted from infiltrating immune cells and inflammatory neutrophils, hepatocyte apoptotic bodies, endothelial cell-mediated growth factors, and reactive oxygen species (ROS) produced by damaged hepatocytes or macrophages [4]. ROS production is an essential feature of activated HSCs, accompanied by the upregulation of NADPH oxidase (NOX) induced by profibrotic factors, such as transforming growth factor-beta 1 (TGF- $\beta$ 1), leptin, angiotensin II, and platelet-derived growth factor (PDGF), which induce the activation of the mitogen-activated protein kinase (MAPK)/extracellular signal-regulated kinase pathway [5]. Increased ROS production by HSCs stimulates the alpha-1 type I collagen (*COL1A1*) promoter, leading to increased collagen production [6], and the knockdown of NOX enzymes reduces HSC activation and liver fibrosis in mice [7]. Therefore, intracellular ROS in HSCs is considered a promising target for many antifibrotic therapies.

Globins are characterized by a 3-on-3 sandwich of  $\alpha$ -helices, known as the globin-fold, and the presence of a heme prosthetic group [8]. In humans, the main four members of globin family have been extensively studied: hemoglobin (HB), myoglobin (MB), neuroglobin (NGB), cytoglobin (CYGB). HB and MB were first described more than 50 years ago, followed by the discovery of NGB in 2000 [9] and CYGB in 2001 [10]. The predominant adult forms of HB feature a heterotetrameric  $\alpha_2\beta_2$  structure, consisting of two  $\alpha$ -subunits (Hb $\alpha$ , encoded by *HBA*) and two  $\beta$ -subunits (Hb $\beta$ , encoded by *HBB*), with each subunit bound to a heme prosthetic group [11]. By contrast, MB, NGB, and CYGB are typically detected in the monomeric state. In addition, both CYGB and NGB contain cysteine residues that form intramolecular disulfide bonds: between Cys46 and Cys55 in NGB and between Cys38 and Cys83 in CYGB [12,13]. These disulfide bonds may be involved in regulating the binding of exogenous ligands to NGB and CYGB and modulating nitrite reductase or ROS scavenging activities [14]. These four globins are reported to be involved in the intracellular regulation of ROS homeostasis, particularly the inhibition of ROS generation and protection against ROS

[8].

Our previous studies reported the role of CYGB, which is exclusively expressed in HSCs. CYGB knockdown promoted fibrosis development during bile duct ligation-induced cholestasis [15], whereas the selective upregulation of CYGB in HSCs attenuated liver injury and collagen accumulation [16]. Extracellular administration of CYGB attenuated HSC activation by ROS scavenging activity and the induction of interferon  $\beta$  and suppressed liver fibrosis in several models in mice [17]. These findings prompted us to consider the anti-fibrotic properties of other globins.

Here, we show the effects of MB, NGB, HB, and CYGB on the activation status of a human HSC cell line, HHSteC, and in a carbon tetrachloride (CCl<sub>4</sub>)-induced mouse model of liver fibrosis. First, we found that extracellular MB, NGB, and CYGB, but not HB, were endocytosed into HHSteCs, exhibited intracellular ROS scavenging activity, and suppressed *COL1A1* promoter activation. Second, we demonstrated that MB and NGB deactivated HHSteCs and promoted matrix metalloproteinase (MMP)-1 secretion, which is involved in collagen degradation in the ECM. Third, intravenously injected MB, NGB, or CYGB were delivered to hepatic sinusoidal cells in mice and suppressed liver fibrosis induced by CCl<sub>4</sub>. Taken together, these findings expand our knowledge of the effects of extracellular globins on HSC activation and liver fibrosis, suggesting new avenues for globin-based therapy in patients with advanced liver fibrosis.

## 2. Materials and methods

### 2.1. Protein production

Recombinant human (rh) CYGB was produced as described previously [17]. Human MB (#30-AM20) and human HB (#30-1134) were obtained commercially (Fitzgerald, Acton, MA).

#### 2.1.1. Cloning, expression, and purification of rhNGB

cDNA encoding the 151-amino acid sequence of human NGB described previously [18] was incorporated into the pET15b plasmid. Human NGB cDNA was amplified by PCR using oligonucleotide primers designed to incorporate *EcoRI* and *XhoI* restriction sites at the 5' and 3' ends of the gene, respectively. Human NGB cDNA was then cloned into the plasmid pRSET A (#V351-20, Invitrogen, Thermo Fisher Scientific, Carlsbad, CA) and sequenced using an ABI 3730 xl DNA Analyzer (Applied Biosystems, Foster City, CA) to confirm gene insertion with the correct orientation. After transformation into the *Escherichia coli* strain

BL21-AI™ (#C6070-03, Invitrogen), expression of human NGB was induced with 0.2% L-arabinose (#A3256-100G, Sigma-Aldrich Co., St. Louis, MO). Expressed NGB with 6His-tag at N-terminus was purified by immobilized metal ion affinity chromatography using the fast protein liquid chromatography method (ÄKTA pure, GE Healthcare Japan Corporation, Tokyo, Japan), followed by size exclusion chromatography (HiLoad 16/600 Superdex 75 pg, GE Healthcare, Uppsala, Sweden). The final collected protein was stored in buffer (150 mM NaH<sub>2</sub>PO<sub>4</sub>, 50 mM NaCl, and 5% glycerol, pH 7.4).

### 2.1.2. Mutagenesis of recombinant NGB

See Supplementary Materials for details.

### 2.1.3. Animal models

Starting at 8 weeks old, male C57BL/6 mice (SLC, Shizuoka, Japan) received twice-weekly intraperitoneal injections of 0.5 mg/kg body weight (BW) of CCl<sub>4</sub> (Wako, Osaka, Japan) diluted in corn oil (Wako) or a similar volume of corn oil only (Vehicle group) for 6 weeks. During the last 4 weeks of CCl<sub>4</sub> injections, mice were administered MB, NGB, or CYGB in saline at 1 mg/kg BW or a similar volume of normal saline via tail-vein injections twice per week. After anesthetized by intraperitoneal injection of pentobarbital (Somnopenyl, Kyoritsu, Tokyo, Japan) 70 mg/kg BW, mice were euthanized two days after the last injection.

All mice received humane care, according to Guide for the Care and Use of Laboratory Animals, National Institutes of Health. All protocols and experimental procedures were approved by the Institutional Animal Care and Use Committee of Osaka City University and were performed following the guidelines of the National Institutes of Health for the use of animals in research. See Supplementary Materials for details.

## 2.2. Cell culture and treatment

HHStECs were purchased from ScienCell Research Laboratories (San Diego, CA) and cultured in complete stellate cell medium (StECM, ScienCell Research Laboratories) supplemented with 2% fetal bovine serum (FBS, ScienCell Research Laboratories), 1% stellate cell growth supplement (S, ScienCell Research Laboratories), and 1% penicillin-streptomycin (P/S, ScienCell Research Laboratories) at 37 °C in humidified air containing 5% CO<sub>2</sub>. HHStECs were passaged when subconfluent and were used between passages 3–10 for all experiments. See Supplementary Materials for details.

### 2.3. RNA-seq and pathway analysis

RNA was isolated from HHStECs with and without MB or NGB treatment (n = 3 each group) and subjected to RNA sequencing (RNA-seq). Whole-transcriptome sequencing was applied to RNA samples using Illumina platform (Macrogen, Seoul, Korea). All RNA-seq data have been deposited in the Gene Expression Omnibus (GEO) database and can be accessed at GSE190258. See Supplementary Materials for details.

### 2.4. Statistical analysis

Data are expressed as the mean ± standard deviation. Statistical analyses were performed using two-tailed Student's t-tests to compare differences between two unpaired groups. One-way analysis of variance (ANOVA), followed by Dunnett's *post hoc* test, was performed to compare multiple groups with control. Two-way ANOVA, followed by Turkey's HSD test, was performed to compare mean differences between groups. *P* < 0.05 was considered significant. GraphPad Prism, version 8.0 for Windows (GraphPad Prism Software, Inc., San Diego, CA), was used for all analyses.

All information regarding Experimental Methods can be found in Supplementary Materials.

## 3. Results

### 3.1. Distribution of extracellular globins in HHStECs

We previously reported the application of rhCYGB as antifibrotic therapy in HHStECs and in multiple *in vivo* models of advanced liver fibrosis [17]. CYGB belongs to the globin family in mammals; therefore, we compared the functions of other globins, including HB, MB, and NGB, with those of CYGB, including antifibrotic properties and capacities for cellular protection against oxidative stress and chemically induced liver fibrosis.

We first examined the safety of purified globins by adding them to the culture medium of HHStECs at concentrations as high as 4 μM and observed no induction of cellular damage, as indicated by lactate dehydrogenase assay (Supplementary Fig. 1A). As shown in Fig. 1A, at 24 h after the addition to the culture medium at 2 μM, MB, NGB, or CYGB, but not HB, localized to the membranous, cytoplasmic, nuclear, and cytoskeletal fractions of HHStECs. The proportion of extracellular globins that translocated into HHStECs was highest for CYGB (566 pg/g total protein), followed by NGB (100 pg/g) and MB (3.4 pg/g) (Fig. 1B).

HB is formed as a tetramer, whereas the other three globins exist as monomeric proteins; therefore, we hypothesize that the bulky structure of HB prevented cellular penetration. However, the mechanism through which exogenous MB, NGB, and CYGB enter cells remains unknown. Our previous work showed that rhCYGB enters cells through clathrin-mediated endocytosis [17]. Since we obtained non-labeled, commercially-available MB, which is unable to be traced under fluorescence microscopy, NGB was employed to clarify the endocytosis mechanism. Fig. 1C and D shows Alexa 488-labeled NGB applied to HHStECs at 0.5 μM for 24 or 48 h could be detected in the HHStEC cytoplasm, but this localization was inhibited by treatment with 10 μM chlorpromazine (CPZ), a clathrin inhibitor or 1000 μM amiloride, a macropinocytosis inhibitor, but not by 10 μM nystatin, a caveola inhibitor (Fig. 1E and F and Supplementary Figs. 1B and C). These data suggest that clathrin- and macropinocytosis-mediated endocytosis pathways are involved in the translocation of extracellular NGB into cells.

### 3.2. Extracellular globins suppress collagen production in HHStECs under conditions of spontaneous and TGF-β1-induced activation

Next, we evaluated the effects of extracellular globins on cultured HHStEC phenotype. Under spontaneously activated conditions, MB, NGB, or CYGB addition (0.25–4 μM, 48 h) markedly suppressed COL1A1 production in HHStECs at both the protein and mRNA levels. NGB had the strongest effect, with a half-maximal inhibitory concentration (IC<sub>50</sub>) of approximately 0.6 μM, followed by MB and CYGB (IC<sub>50</sub> values of 1.24 and 2.4 μM, respectively) (Fig. 2A, B, and D). The COL1A1 suppressive effects of globin treatment could be observed starting 24 h after incubation (Supplementary Fig. 2A). To clarify the role of internalized globins in maintaining COL1A1 suppression, HHStECs were treated with NGB, the most potent inhibitor (Fig. 2B), for 48 h. Successive removal of NGB-containing medium and replacement with fresh medium caused intracellular NGB levels to decrease in a time-dependent manner, and COL1A1 expression increased in both cell lysate and medium (Supplementary Fig. 2B). Consistent with the inability of HB to penetrate the cell, HB treatment resulted in only a mild reduction in COL1A1 expression at the mRNA level without changing protein levels (Fig. 2C). Following stimulation of HHStECs with 2 ng/mL TGF-β1 for 48 h, 2 μM MB, NGB, or CYGB, but not HB, inhibited COL1A1 production (Fig. 2E) with a similar capacity as observed for spontaneous activation (Fig. 2F). These results indicated that except for HB, all globins inhibited COL1A1 synthesis in HHStECs under both spontaneously activated and TGF-β1-stimulated conditions. Although CYGB effectively suppressed α-smooth muscle actin (αSMA) expression (Fig. 2B), consistent with previous observations [17], MB and NGB exhibited limited regulation of αSMA expression. Therefore, we focused our analyses on the MB- and

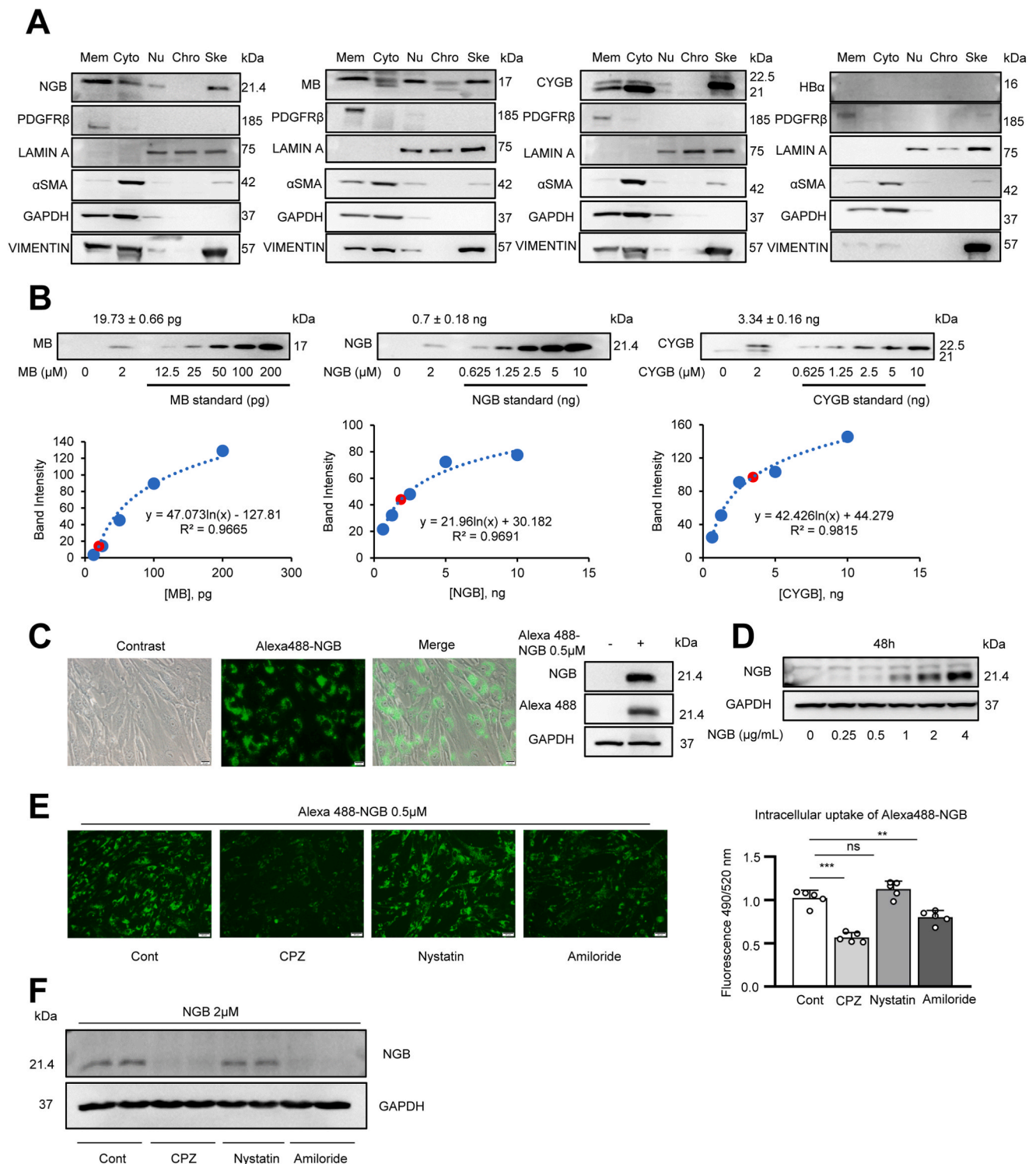


**Fig. 1. Distribution of extracellular globins in HHStECs.** (A) Immunoblotting analysis for fractionated cellular proteins in HHStECs treated with globins. Marker for cytoplasmic (Cyto): GAPDH, plasma membrane (Mem): PDGFR $\beta$ , nuclear soluble (Nu) and chromatin-bound (Chro): LAMIN A and cytoskeletal (Ske):  $\alpha$ SMA, VIMENTIN. (B) Immunoblotting analysis (top) for MB, NGB, CYGB expression in untreated and MB, NGB, or CYGB-treated HHStEC cell lysate alongside their standards. A total of 6  $\mu$ g protein of HHStEC cell lysate was loaded. Quantification of protein content from blot (mean  $\pm$  sd) (bottom panels). A calibration curve was plotted from densities of globin standards (blue dot) and used to determine the amount of MB, NGB, or CYGB (2  $\mu$ M, 48 h) translocated into HHStECs (red dot). (C) Representative fluorescent images and immunoblotting analysis of the intracellular distribution of Alexa 488-NGB (green, 0.5  $\mu$ M, 48 h) in HHStECs. Bars 20  $\mu$ m. (D) Immunoblotting analysis for dose-dependently NGB treatment in HHStECs. (E) Representative fluorescent images (left panel) for endocytosis inhibitor assay with their relative absorbance (right panel). Inhibitors of clathrin-mediated endocytosis (chlorpromazine, CPZ), caveolae-mediated endocytosis (nystatin), or macropinocytosis (amiloride) were pre-treated for 3 h, followed by Alexa 488-NGB treatment for next 4 h ( $n = 5$ ). (F) Effect of endocytosis inhibitors on cellular uptake of NGB in HHStECs. Immunoblotting analysis for HHStECs untreated (Cont) or pre-treated with inhibitors of CPZ, nystatin, and amiloride for 3 h, then NGB (2  $\mu$ M) treated for 4 h ns, not significant,  $*P < 0.05$ ,  $**P < 0.01$ ,  $***P < 0.001$ , one-way ANOVA followed by Dunnett's *post hoc* test. Data (A–F) are representative of three independent experiments. (For interpretation of the references to color in this figure legend, the reader is referred to the Web version of this article.)

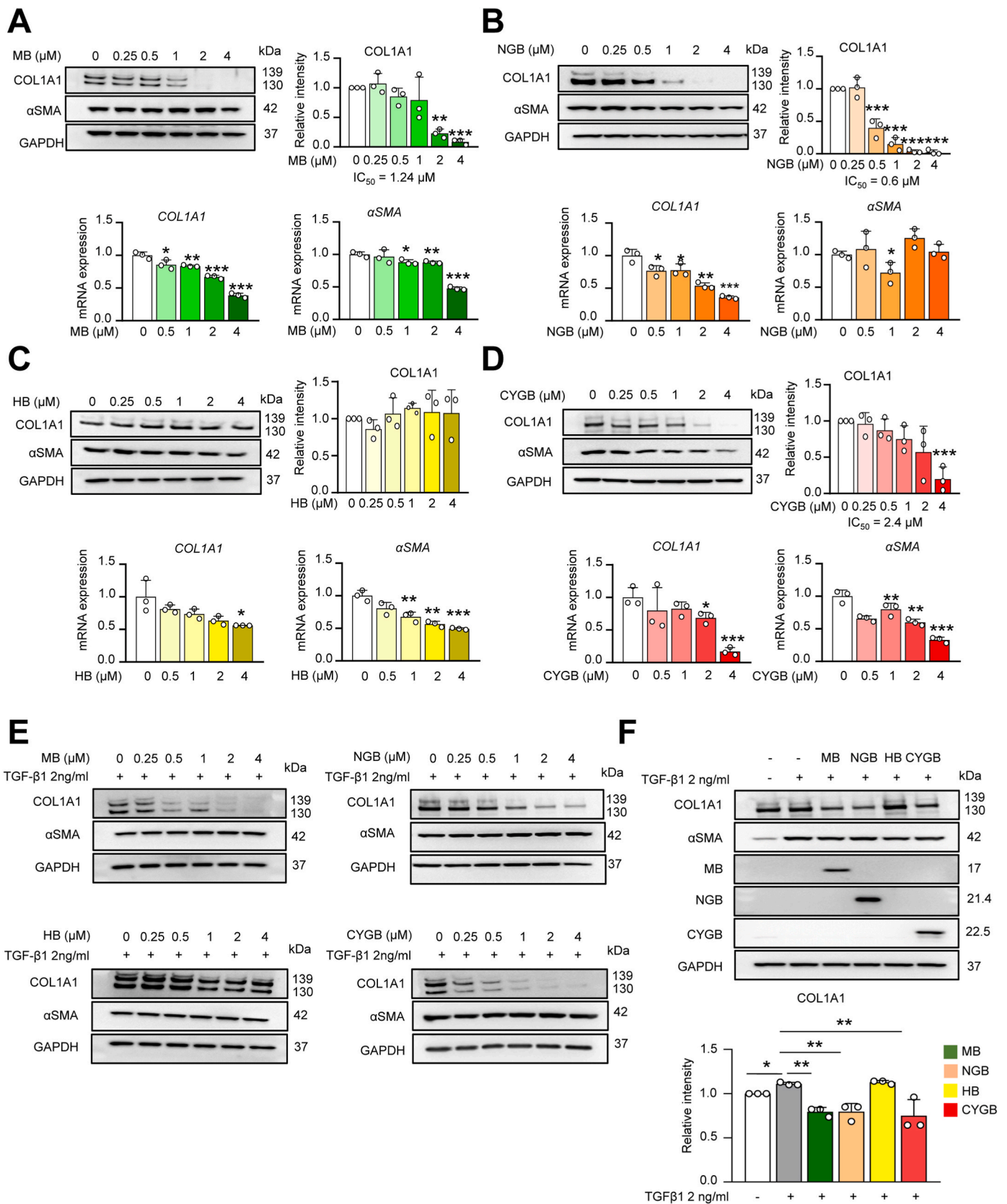


**Fig. 2. Extracellular globins suppress collagen production in HHStECs under conditions of spontaneous and TGF-β1-induced activation.** (A–D) Immunoblotting analysis for COL1A1 with band density quantifications and αSMA expression of activated HHStECs following MB, NGB, HB, and CYGB treatment dose-dependently for 48 h (top panels), and their qRT-PCR analysis (bottom panels). (E) Immunoblotting analysis for HHStECs which were co-treated with TGF-β1 (2 ng/mL) and globins dose-dependently for 48 h: MB (top-left panel), NGB (top-right panel), HB (bottom-left panel), and CYGB (bottom-right panel). (F) Immunoblotting analysis (top panel) and band density quantification for COL1A1 expression (bottom panel) in HHStECs co-treated with TGF-β1 (2 ng/mL) and globins (2 μM) for 48 h \*P < 0.05, \*\*P < 0.01, \*\*\*P < 0.001. One-way ANOVA followed by Dunnett’s *post hoc* test.

NGB-mediated regulation of COL1A1 expression in HHStECs, using CYGB as the positive control.

### 3.3. Intracellular ROS-scavenging capacity of globins suppresses COL1A1 promoter activity

Heme-binding proteins are known for detoxifying ROS, including  $O_2^{\bullet-}$ ,  $OH^{\bullet}$ , and  $H_2O_2$  [8], which is expected to suppress COL1A1 synthesis. In a cell-free system, all globins displayed reduced and oxidized pyridine hemochromogen at 50  $\mu$ M, which is characteristic of heme-containing proteins (Supplementary Fig. 3A). Based on the Trolox (vitamin E) equivalent capacity of cupric reduction (see Supplementary Materials and Methods for details), the total antioxidant capacities of 1  $\mu$ M HB, NGB, CYGB, and MB were measured at 4.5 mM, 3.4 mM, 2.0 mM, and 0.7 mM Trolox equivalents, respectively, which were higher than the capacity of 1  $\mu$ M glutathione (0.5 mM Trolox, Fig. 3A). We evaluated the ability of globins to scavenge  $O_2^{\bullet-}$  generated by hypoxanthine-xanthine oxidase in a cell-free system using the Besso assay (Fig. 3B, left panel). MB and HB showed  $IC_{50}$  values of 0.44 and 0.55  $\mu$ M, respectively, which were 3-fold and 37-fold lower than those for CYGB and NGB, respectively (Fig. 3B, right panel). All globins showed stronger  $O_2^{\bullet-}$ -scavenging ability than vitamin C, a well-known antioxidant.

The spontaneous activation of HHStECs in cell culture resulted in increased cellular ROS formation over time, as measured using a 2',7'-dichlorofluorescein diacetate (DCFDA)-based assay after 24 and 48 h of culture. Increased ROS was suppressed by treatment with 4  $\mu$ M MB, NGB, or CYGB, but not HB (Fig. 3C, left panel). We stimulated HHStECs with a ROS inducer, *tert*-butyl hydroperoxide (TBHP), an organic  $H_2O_2$  compound, and measured ROS generation using either the DCFDA assay (Fig. 3C, right panel) or the Bes- $H_2O_2$  assay (to specifically detect  $H_2O_2$ ) (Fig. 3D and E, Supplementary Fig. 3B). These two assays demonstrated the ROS-scavenging capacities of MB, NGB, and CYGB, but not HB. Although all four globins revealed ROS-scavenging and antioxidant functions in a cell-free system, MB, NGB, and CYGB were able to scavenge intracellular ROS formation, whereas HB did not.

These results led to the question of how the ROS-scavenging function of globins attenuates COL1A1 production in HHStECs. We examined human *COL1A1* promoter activity under globin-treated conditions in spontaneously activated HHStECs and found, as expected, that MB, NGB, and CYGB, but not HB, suppressed human *COL1A1* promoter activity in a time-dependent manner (Fig. 3F).

When HHStECs were challenged with TBHP for 0–48 h, *COL1A1* promoter activity increased, peaking at 8 h (Fig. 3G, top panel). This activity decreased when HHStECs were co-treated with TBHP and MB, NGB, or CYGB, but not HB (Fig. 3G, bottom panel). Consistent with these results, stimulation of HHStECs with TBHP induced upregulation of COL1A1 protein levels in time- and dose-dependent manners (Fig. 3H, top and middle panel), which could be suppressed by treatment with 4  $\mu$ M MB, NGB, or CYGB, but not HB (Fig. 3H, bottom panel). We further verified these results using TGF- $\beta$ 1-stimulated HHStECs. TGF- $\beta$ 1 induced ROS formation in HHStECs in a dose-dependent manner for 48 h (Fig. 3I, left panel) which were blunted by treatment with MB, NGB, or CYGB, but not HB (Fig. 3I, right panel). Thus, the intracellular ROS-scavenging capacity of MB, NGB, and CYGB, but not HB, resulted in the inhibition of *COL1A1* gene promoter activity. Accordingly, we excluded HB from further evaluations.

### 3.4. Modifying the structure of globins affects their ability to scavenge ROS

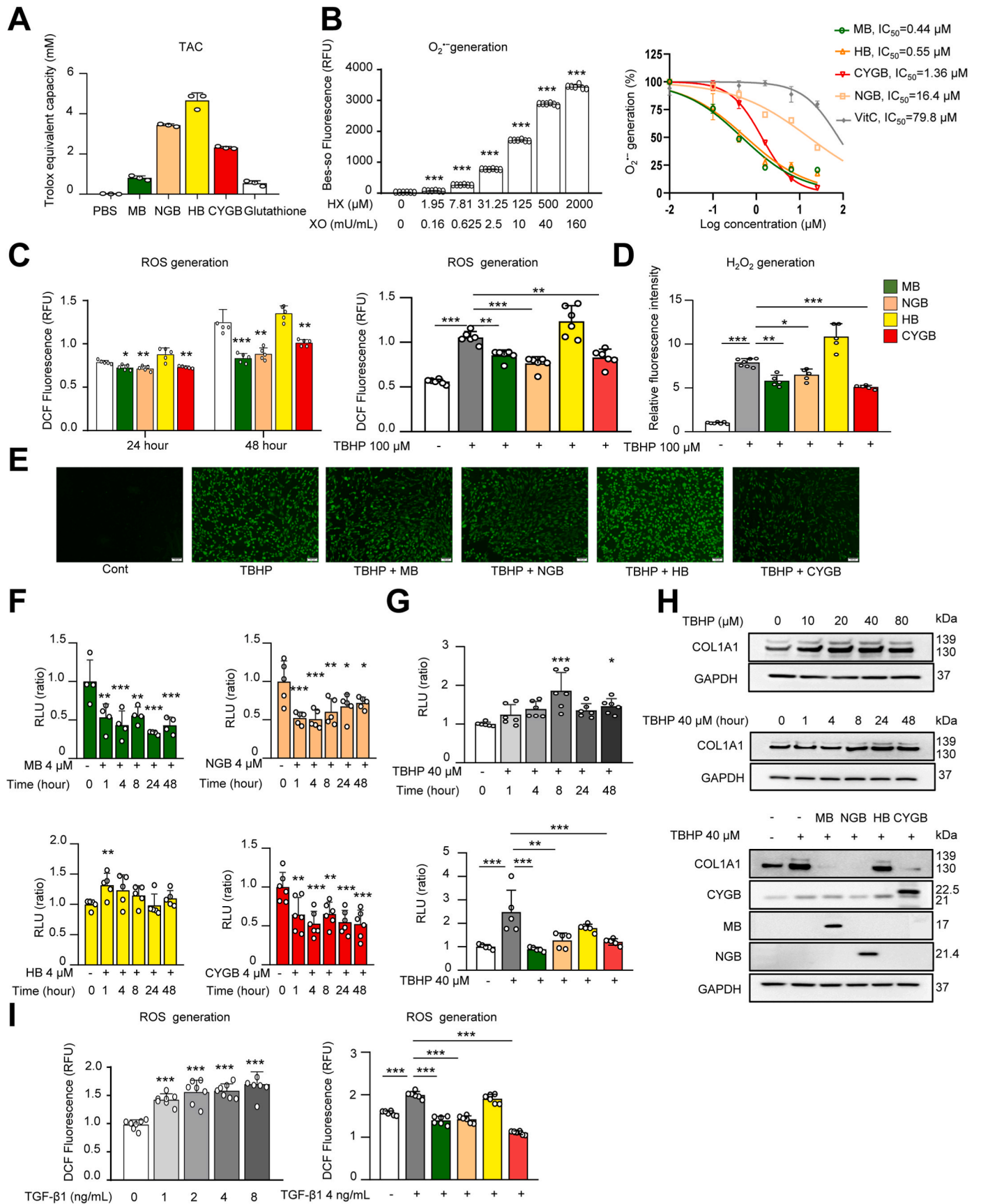
Several studies report that key structural features of globins regulate their functions [13,18]. The role of globins in the inhibition of COL1A1 synthesis appears closely related to the redox and ligation states of the heme-bound iron [12]. Because we produced rhNGB in-house, we were able to modify the structure, unlike the commercially obtained MB.

Therefore, we studied this issue using NGB as a representative sample. His96 is known to serve as a proximal ligand in NGB, and, therefore, we replaced this amino acid with alanine, which is unable to coordinate the iron molecule (Supplementary Fig. 4A). The motility of purified H96A mutant, when assessed by sodium dodecyl sulfate–polyacrylamide gel electrophoresis, was similar to that of the wild-type (WT) NGB (Fig. 4A). The mutant NGB is colorless, indicating the complete absence of heme (Fig. 4B). However, unexpectedly, H96A mutant retained  $O_2^{\bullet-}$ -scavenging activity (Fig. 4C) and suppressed COL1A1 expression at both the protein (Fig. 4D, left and middle panels) and mRNA levels (Fig. 4D, right panel), with an  $IC_{50}$  similar to that for WT NGB (0.59  $\mu$ M and 0.6  $\mu$ M, respectively).

Unlike MB and HB, NGB and CYGB contain cysteine residues that form an intramolecular disulfide bridge [13,19]. As reported [19], the Cys46/Cys55 disulfide bond influenced the redox and spectroscopic properties of human NGB. Therefore, we substituted Cys46 and Cys55 with Gly46 and Ser55, respectively, disrupting the disulfide bond between Cys46 and Cys55 in NGB (Fig. 4E, left panel, Supplementary Fig. 4B). This SH–SH mutant demonstrated decreased heme activity (Fig. 4E, right panel) and reduced  $O_2^{\bullet-}$ -scavenging activity (Fig. 4F). In addition, this SH–SH mutant significantly attenuated capacity to inhibit COL1A1 production with an  $IC_{50}$  of 2.15  $\mu$ M (Fig. 4G) compared with the  $IC_{50}$  of 0.6  $\mu$ M for WT NGB. Thus, single structural mutations, such as H96A or C46G–C55S, can partially modify the function of NGB but do not result in the complete loss of function. These characteristics of NGB differ from those of CYGB because the replacement of the Fe center with a Co molecule in the heme group of CYGB completely disrupted CYGB function, as shown in our previous study [17].

### 3.5. MB and NGB downregulate fibrosis-related genes and induce HHStEC deactivation and MMP-1 secretion

Previously, we performed RNA-seq analysis in rhCYGB-treated HHStECs compared with untreated controls and showed that rhCYGB treatment inhibited fibrosis-related pathways and stimulated interferon (IFN)  $\beta$ 1 secretion [17]. We investigated the common and differential pathways activated in HHStECs treated with 4  $\mu$ M MB or NGB ( $n = 3$ , each group). The RNA-seq data revealed that 2977 and 1637 genes were significantly changed by 2-fold or greater ( $p < 0.05$ ) in the MB and NGB treatment groups, respectively, compared with untreated controls (Supplementary Fig. 5A). Consistent with the results observed following rhCYGB treatment [17], RNA-seq analysis revealed the downregulation of ECM-encoding and fibrosis-related genes, such as *COL1A2*, *COL3A1*, *PDGFR $\alpha$* , and *S100A4*, and the upregulation of transcription factors that regulate the deactivation phenotype of HHStECs, including Peroxisome proliferator-activated receptor gamma (*PPAR $\gamma$* ), E26 transcription-specific (*ETS*) 1, *ETS2*, and Interferon regulatory factor (*IRF*) 1 (Fig. 5A). These findings were confirmed by quantitative reverse transcriptase-polymerase chain reaction (qRT-PCR; Fig. 5B and C). Pathway analysis of the MB and NGB treatment groups revealed 633 commonly downregulated genes (Supplementary Fig. 5B), with TGF- $\beta$  regulation of the ECM identified as the most downregulated pathway (Supplementary Fig. 5C). Surprisingly, MB and NGB also promoted the upregulation of MMP genes involved in collagen degradation in the ECM (Fig. 5A). Both MB and NGB treatment induced MMP-1 mRNA expression in a dose-dependent manner in cultured HHStECs (Fig. 5D, left panel), which was accompanied by an increase in MMP-1 secretion, as measured in the culture medium (Fig. 5D, right panel), indicating that MMP-1 might serve as an upstream regulator of collagen reduction in the extracellular environment of HHStECs (Supplementary Fig. 5D). MMP-1 knockdown by small interfering RNA (siRNA; 5 pM for 24 h; Fig. 5E) showed no effects on intracellular COL1A1 levels in HHStECs treated with 4  $\mu$ M NGB (Fig. 5F, left panel), but partially reversed the reduction of COL1A1 levels in the extracellular medium compared with the control siRNA (Fig. 5F, right panel). These results suggested that MMP-1 was involved in the observed reduction of COL1A1 in the



(caption on next page)

**Fig. 3. Intracellular ROS-scavenging capacity of globins suppresses COL1A1 promoter activity.** (A) Total antioxidant capacity (TAC) of Phosphate-Buffered Saline (PBS), MB, NGB, HB, CYGB, and Glutathione at 1  $\mu$ M in a cell-free system. (B) Determination of  $O_2^{\bullet-}$  generation by BES-So assay in a cell-free system. The left panel showed Hypoxanthine-Xanthine oxidase (HX-XO) reaction induced  $O_2^{\bullet-}$  generation in a dose-dependent manner. The right panel showed MB, NGB, HB, CYGB, and ascorbic acid (Vitamin C) dose-dependently scavenged  $O_2^{\bullet-}$  generated by HX (125  $\mu$ M) and XO (10mU/mL) challenge.  $IC_{50}$ , the half-maximal inhibitory concentration. (C) Determination of intracellular ROS by DCFDA assay in activated HHStECs under spontaneous condition with globin treatment 24 and 48 h (left panel) and in HHStECs induced with *tert*-butyl hydroperoxide (TBHP, 100  $\mu$ M, 1 h), which were pre-treated with globins (4  $\mu$ M, 24 h) (right panel). RFU, relative fluorescence unit. (D, E) Determination of fluorescent intensity and representative images of intracellular  $H_2O_2$  generation by Bes- $H_2O_2$  assay in HHStECs pre-treated with globins (4  $\mu$ M, 24 h), followed by TBHP (100  $\mu$ M, 1 h) treatment. (F) COL1A1 promoter activity was measured by Dual-Luciferase reporter assay in HHStECs transfected with COL1A1 promoter construct for 24 h and then treated with MB, NGB, HB, and CYGB (4  $\mu$ M) time-dependently. RLU, relative light unit. (G) COL1A1 promoter activity was measured by Dual-Luciferase reporter assay in HHStECs which were transfected with COL1A1 promoter construct for 24 h and then treated with TBHP (40  $\mu$ M) in a time-dependent manner (top panel) or co-treated globins (4  $\mu$ M) and TBHP (40  $\mu$ M) for 8 h (bottom panel). (H) Immunoblotting analysis of activated HHStECs under dose-dependent treatment of TBHP for 48 h (top panel) or time-dependent treatment of TBHP (40  $\mu$ M) (middle panel), and TBHP-induced activated HHStECs without or with globins pre-treatment (2  $\mu$ M, 24 h) (bottom panel). (I) Determination of intracellular ROS generation by DCFDA assay in HHStECs treated with TGF- $\beta$ 1 in a dose-dependent manner for 48 h (left panel) and in HHStECs pre-treated with globins at 4  $\mu$ M for 24 h, followed by TGF- $\beta$ 1 (4 ng/mL) for 8 h (right panel). \* $P < 0.05$ , \*\* $P < 0.01$ , \*\*\* $P < 0.001$ . One-way ANOVA followed by Dunnett's *post hoc* test.

extracellular microenvironment following NGB and MB treatment.

Next, we evaluated specific upregulated genes in NGB-treated HHStECs. NGB treatment specifically upregulated 226 genes, with the most significantly enriched pathway identified as Interferon (IFN)  $\alpha/\beta$  signaling (Supplementary Fig. 6A). The heatmap generated using RNA-seq data showed that NGB treatment upregulated IFN-stimulated genes, including Interferon Alpha Inducible Protein (*IFI*) 27, *IFI6*, Interferon-stimulated gene (*ISG*) 15, IFN-regulatory factors (*IRF*) 7, *IRF9*, and 2'-5'-oligoadenylate synthetase (*OAS*) 2 (Supplementary Fig. 6B), which was confirmed by qRT-PCR (Supplementary Fig. 6C). At the protein level, 4–8 h of NGB treatment induced the phosphorylation of signal transducer and activator of transcription 1 (Supplementary Fig. 6D). Taken together, it was evident that NGB effects on gene expression of HHStECs is analogous to the effects observed for rhCYGB [17].

### 3.6. Distribution and safety of globins in vivo

We examined the biodistribution of NGB, as a representative globin, following intravenous injection into normal mice. The *in vivo* and *ex vivo* analysis of Alexa 488-conjugated NGB (Alexa 488-NGB) revealed significant fluorescent signal accumulation in the liver, kidney, spleen, intestine, stomach, and bladder of WT mice 1 h after injection (Fig. 6A). To our surprise, at the tissue level, immunohistochemical analysis revealed Alexa 488-NGB localization in hepatic sinusoidal cells, proximal tubular region of the kidney, splenic sinusoidal cells in the red pulp of spleen, and periacinar cells in the pancreas (Fig. 6B). Further analysis using double immunohistochemical staining indicated that Alexa 488-NGB co-localized with HSC marker desmin and endothelial cell marker CD31, but not macrophage marker CD68 (Fig. 6C).

We then investigated NGB biodistribution in a 6-week CCL<sub>4</sub>-induced liver fibrosis mouse model. We used 5 nm Ni-NTA nanogold particles to label injected His-tagged NGB proteins using a post-embedding labeling method and observed NGB localization by transmission electron microscopy (TEM). No signals of nanogold particles were found in liver sections without His-tagged NGB treatment (Supplementary Fig. 7A). Consistent with the distribution of Alexa 488-NGB in normal mice, nanogold-labeled NGB localized predominantly to the HSC cytoplasm (Fig. 6D, left panel) in addition to endothelial cells (Fig. 6D, right panel) and hepatocytes (Supplementary Fig. 7B) in mouse fibrotic liver.

### 3.7. MB, NGB, or CYGB administration prevented the aggravation of CCL<sub>4</sub>-induced liver fibrosis

The applicability of MB, NGB, or CYGB as protein therapies against liver injury and fibrosis was tested using an *in vivo* mouse model. All globins at 1 mg/kg BW were administered by intravenous injection twice per week during the last four weeks of the 6-week liver fibrosis model induction protocol using CCL<sub>4</sub> (Supplementary Fig. 8). The biochemical analysis of aspartate aminotransferase (AST), alanine aminotransferase (ALT) in the blood showed no aggravation of liver

function (Fig. 7A). Serum creatinine was also not different among groups. Serum levels of AST and ALT were shown to be significantly reduced by administration of CYGB, but not MB or NGB (Fig. 7A). Six weeks of CCL<sub>4</sub> treatment induces collagen deposition as indicated by Sirius Red and Fast Green (SiR-FG) staining,  $\alpha$ SMA expression, CD68 macrophage infiltration, and neutrophil populations. Mice treated with MB, NGB, or CYGB exhibited the clear attenuation of these manifestations (Fig. 7B and C). Treatment with these globins also significantly suppressed mRNA levels of fibrosis-related genes, including *Col1a1*,  *$\alpha$ Sma*, *Pdgfr $\beta$* , *Timp1*, and *Tgf- $\beta$ 1* (Fig. 7D) and inflammatory-related genes, such as *Cxcl-2* and *Ccl3* (Fig. 7E). Hydroxyproline measurements indicated significantly reduced collagen contents in liver tissues from all globin-treated groups compared with those in the control group (Fig. 7F). The levels of lipid peroxidation, 4-hydroxynonenal (4-HNE), were significantly reduced following MB, NGB, or CYGB treatment (Fig. 7B and C). These findings indicate that administration of MB, NGB, and CYGB attenuated fibro-inflammatory reaction in CCL<sub>4</sub>-induced liver injury model.

## 4. Discussion

The functions of globin members have been extensively studied, focusing primarily on the specific tissues where the proteins are expressed (i.e., MB in muscle, NGB in nervous tissues, and CYGB in pericytes and fibroblasts) [8]. Beyond the well-established respiratory functions of heme-containing proteins, all globins are also involved in the regulation of ROS homeostasis and cellular protection from oxidative stress [8]. By contrast, the tumor-suppressive functions of MB [20] and CYGB [21] have also been reported in several types of cancer. To the best of our knowledge, the extracellular effects of globins other than CYGB on liver fibrosis and HSC activation induced by chemicals or ROS insults have remained unexplored. Our current study showed that MB, NGB, HB, and CYGB displayed high ROS-scavenging capacities, similar to previous reports [22], and MB, NGB, and CYGB were unexpectedly able to be internalized into HHStECs via the endocytosis pathway, localizing primarily to membranes, cytoplasm, and cytoskeleton. The inability of HB to be internalized might be associated with specific structural features, as native HB exists in a tetrameric form, whereas MB, NGB, and CYGB exist in a monomeric form [11,23]. Intracellular  $H_2O_2$  generation induced by TGF- $\beta$ 1 stimulation is known to accelerate the binding of the transcription factor C/EBP $\beta$  to its cognate element on the *COL1A1* promoter [6]. We verified that ROS production increased *COL1A1* promoter transactivation, accelerating collagen production in HHStECs, and extracellularly administered globins scavenged ROS, thereby subsequently inhibited *COL1A1* expression. In an *in vivo* CCL<sub>4</sub>-induced liver injury model, administration of exogenous MB, NGB, or CYGB significantly suppressed inflammation and liver fibrosis development, coinciding with the inhibition of 4-HNE, the oxidative stress marker with strong pro-fibrogenic activity on HSCs, also based on ROS scavenging function.

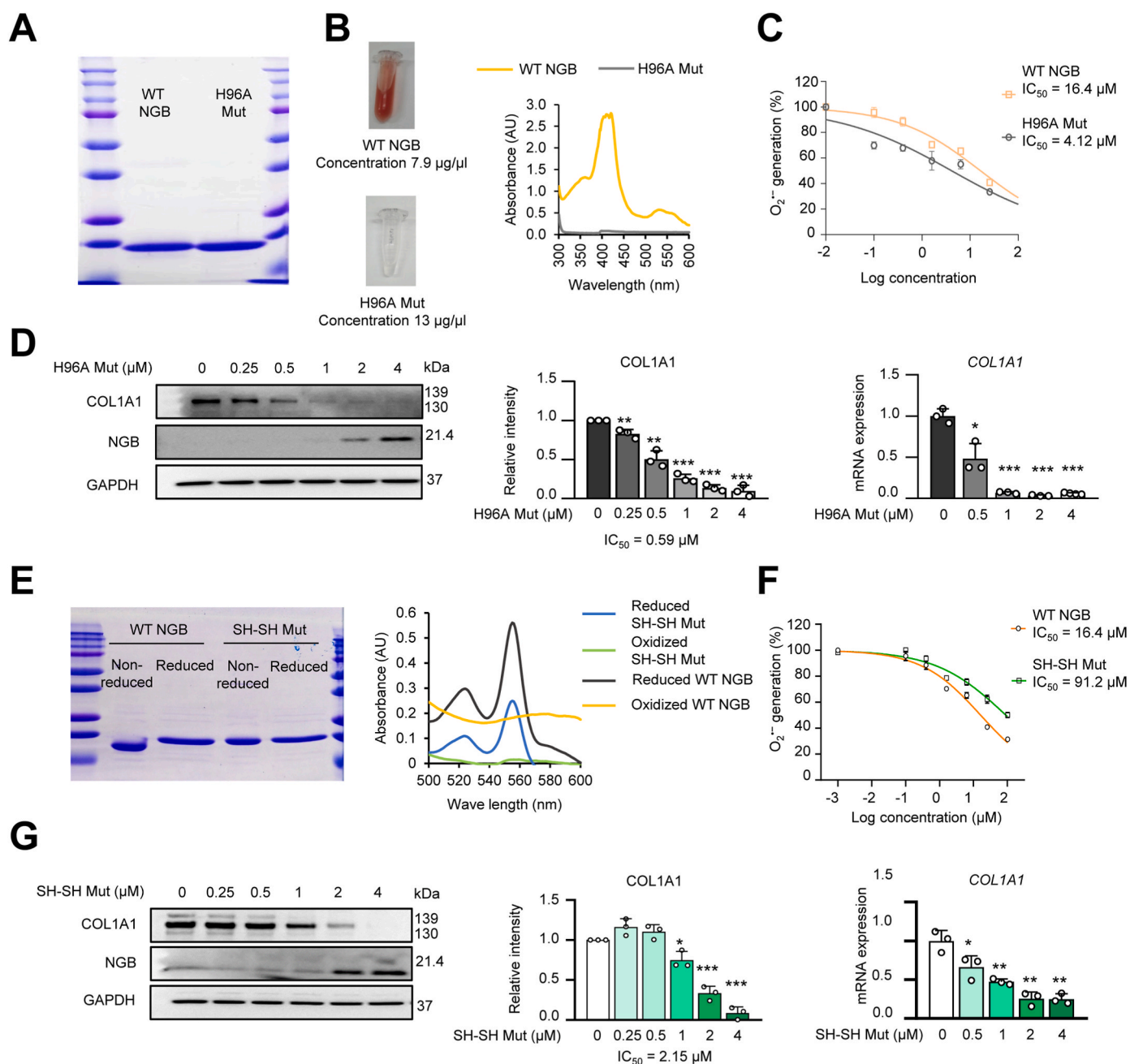


**Fig. 4. Modifying the structure of globins affects their ability to scavenge ROS.** (A) Sodium dodecyl sulfate–polyacrylamide gel electrophoresis (SDS–PAGE) of Wild-type (WT) NGB and H96A Mutant (H96A Mut). (B) WT NGB and H96A Mut protein color and their heme absorbance. (C) WT NGB and H96A Mut dose-dependently scavenged O<sub>2</sub><sup>•-</sup> generated by Hypoxanthine (HX, 125 µM) and Xanthine oxidase (XO, 10mU/mL) challenge. IC<sub>50</sub>, the half-maximal inhibitory concentration. (D) Immunoblotting analysis with band density quantification for COL1A1 expression (left and middle panels), and qRT–PCR analysis of activated HHStECs treated with H96A Mut dose-dependently (right panel). (E) SDS–PAGE of WT NGB and SH-SH Mutant (SH-SH Mut) under non-reduced and Dithiothreitol (DTT)-reduced condition (left panel). The spectrum of reduced and oxidized pyridine hemochromogen of WT NGB and SH-SH Mutant (right panel). (F) WT NGB and SH-SH Mut dose-dependently scavenged O<sub>2</sub><sup>•-</sup> generated by HX (125 µM) and XO (10mU/mL) challenge. (G) Immunoblotting analysis and band density quantifications for COL1A1 (left and middle panels), and qRT–PCR analysis of activated HHStECs treated with SH-SH Mut dose-dependently (right panel). \**P* < 0.05, \*\**P* < 0.01, \*\*\**P* < 0.001. One-way ANOVA followed by Dunnett’s *post hoc* test. (For interpretation of the references to color in this figure legend, the reader is referred to the Web version of this article.)

Recent scientific advances have facilitated the development of novel protein-based products to exploit their innate biological activities [24]. Protein therapies present several advantages over small-molecule, drug-based therapies: 1) proteins can perform highly specific and complex functions; 2) proteins are less likely to interfere with normal body processes or cause side effects; 3) protein therapy is less likely to elicit an immune response; and 4) protein therapy is safer than gene therapy because genome modifications can cause tumorigenesis [24]. Albumin is

a protein produced by hepatocytes with many functional properties, resulting in its broad application [25]. Maeda et al., in 2015, showed that polythiolated and mannosylated recombinant human serum albumin displayed significant hepatoprotective activities against chemically induced hepatitis [26]. Among globins, HB was used to attenuate hepatic injury due to ischemia/reperfusion in a study showing that carbon monoxide-bound HB vesicles infused into rats with hemorrhagic shock improved oxidative damage in the liver [27]. However, available

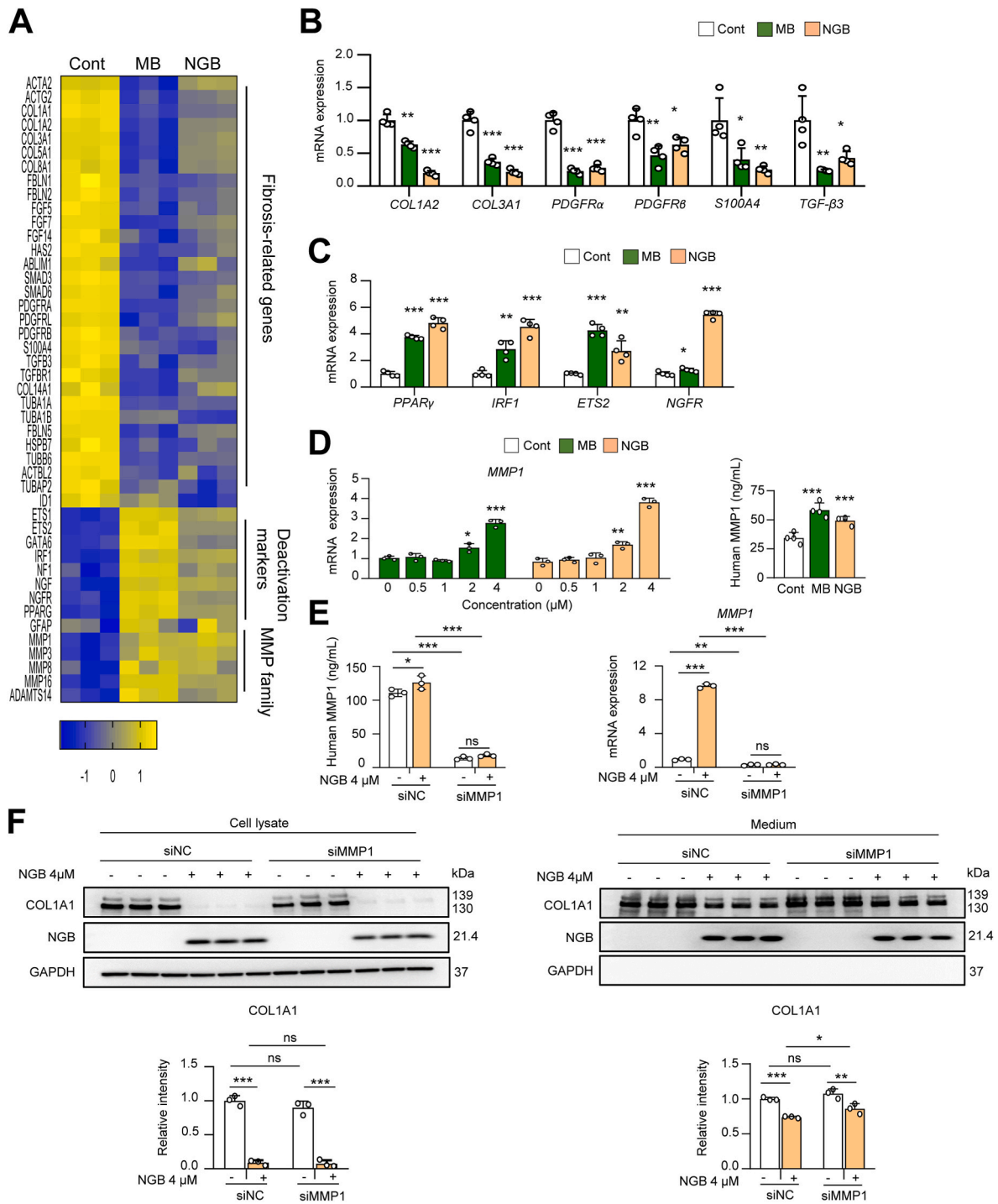


**Fig. 5. MB and NGB downregulate fibrosis-related genes and induce HHStEC deactivation and MMP-1 secretion.** (A) Heatmap analysis of fibrosis-related genes, HSC deactivation-related genes, and MMP family genes which were significantly changed in HHStECs treated with MB or NGB (4  $\mu$ M, 48 h) compared to untreated controls (Cont) by RNA-Seq (n = 3). (B–C) qRT-PCR analysis of genes related to fibrosis (B) and HSC deactivation (C) which were significantly changed in HHStECs treated with MB or NGB (4  $\mu$ M, 48 h) compared to untreated control. (D) MMP-1 mRNA expression in HHStECs treated dose-dependently with MB or NGB (left panel) and measurement of human MMP-1 protein in cultured media of MB or NGB treated HHStECs (4  $\mu$ M) by ELISA (n = 4) (right panel). (E) Measurement of human MMP-1 protein in cultured media by ELISA (n = 3) (left panel) and qRT-PCR of MMP-1 mRNA expression (right panel) in HHStECs transfected with siRNA negative control (siNC) and siRNA MMP-1 (siMMP1) with and without NGB (4  $\mu$ M, 48 h) treatment (n = 3). (F) Immunoblotting analysis and band density quantifications for COL1A1 expression of HHStECs transfected with siNC and siMMP1 with and without NGB (4  $\mu$ M, 48 h) treatment in the cell lysate (left panel) and culture medium (right panel). Ns, non-significant. \* $P$  < 0.05, \*\* $P$  < 0.01, \*\*\* $P$  < 0.001. Data were analyzed using one-way ANOVA followed by Dunnett's *post hoc* test (A–D), or using two-way ANOVA followed by Turkey's HSD test (E–F).

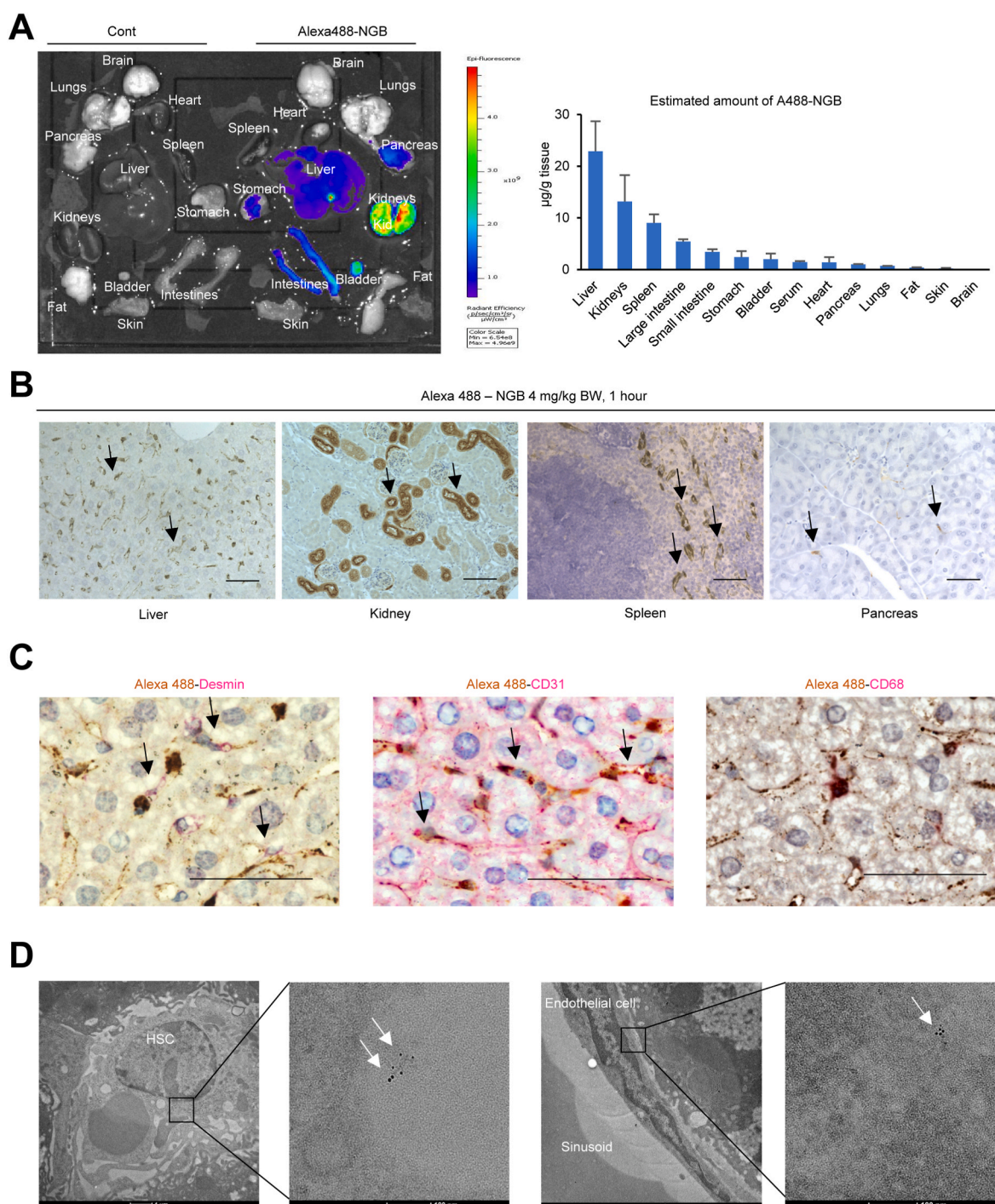


**Fig. 6. Distribution and safety of globins *in vivo*.** (A) Representative fluorescent images of the Alexa 488-NGB detection in normal WT mice at 1 h after injection with 4 mg/kg BW (left panel) and estimated amount of Alexa 488-NGB in different organs (right panel) ( $n = 2$ ). (B) IHC staining for Alexa488-positive cells in the liver, kidney, spleen, and pancreas of WT mice 1 h after injection with 4 mg/kg BW of A488-NGB. Black arrows indicate positive cells. Bars 50  $\mu\text{m}$ . (C) Double IHC staining of Alexa 488 with Desmin, CD31, and CD68. Black arrows indicate double-positive cells. Bars 50  $\mu\text{m}$  (D) Transmission electron microscopic images of the liver section of 6-weeks  $\text{CCl}_4$ -treated mice which were injected with NGB 15 mg/kg BW for 1 h, and then performed post-embedding immunogold labeling assay. Representative images of NGB in HSC (left panel) and endothelial cell (right panel). White arrows indicate nanogold-labeled His-NGB signal. Bars 1  $\mu\text{m}$ .

therapeutic protein options for liver fibrosis remain limited [28]. Our previous study showed that rhCYGB administration in mice effectively reversed liver fibrosis induced by thioacetamide or 3,5-diethoxycarbonyl-1,4-dihydrocollidine [17]. Here, we showed that NGB and MB, similar to CYGB, display antioxidant and ROS-scavenging functions *in vitro* and anti-fibrotic capacities *in vivo*.

The safety of protein therapy is an essential consideration. Excessive

cell-free MB in circulation due to rhabdomyolysis has been associated with nephrotoxicity, progressing to acute renal failure in settings of myoglobinuria [29]. One study reported that intravenously injected MB at a dose of 35 mg/kg BW was compatible with the concentration range observed in rhabdomyolysis [30]. The intravenously injected dose used in our study was 1 mg/kg BW for each globin, which is much lower than the range associated with rhabdomyolysis. CYGB was also reported to be

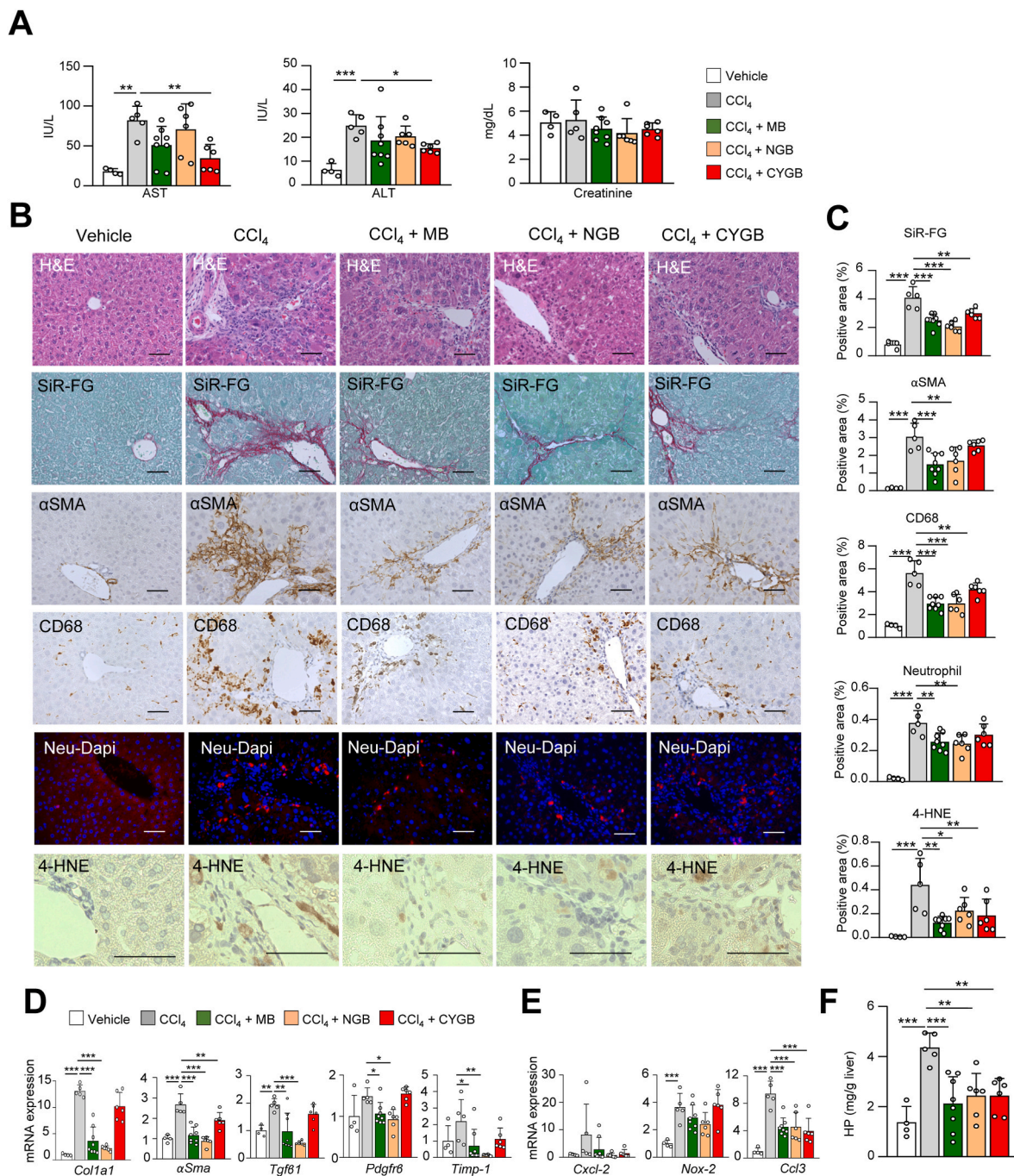


**Fig. 7.** MB, NGB, and CYGB administration prevented the aggravation of CCl<sub>4</sub>-induced liver fibrosis. The experiment design is shown in [Supplementary Fig. 8](#). (A) Serum levels of AST, ALT, and Creatinine. (B–C) Representative liver images of H&E, SiR-FG, IHC staining of αSMA, CD68, 4-HNE (B) and their quantifications (C), n = 4–8. IF staining of neutrophil (Neu – red), Dapi (blue) was used to visualize nuclei and their quantifications n = 4–8. Bars 50 μm. (D–E) qRT-PCR analysis for genes involved in fibrosis (D) and inflammation (E) in the liver (n = 4–8). (F) The amount of hydroxyproline (HP) in the liver (n = 4–8). \**P* < 0.05, \*\**P* < 0.01, \*\*\**P* < 0.001. One-way ANOVA followed by Dunnett's *post hoc* test. (For interpretation of the references to color in this figure legend, the reader is referred to the Web version of this article.)

safe for mice at acute and chronic phases [17]. We propose that low globin concentrations in circulation and specific distribution in liver mesenchymal cells are not likely to cause side effects, supporting the safety of globins.

Antioxidant compounds, including food supplements and drugs, such as polyunsaturated phosphatidylcholine [31] and peroxisome proliferator-activated receptor-α ligand [32] have been evaluated in multiple experimental models of liver fibrosis/cirrhosis. Clinically, the glutathione precursor, N-acetylcysteine, and Mito-TEMPO, an

Mn-superoxide dismutase mimetic, have been used to treat acetaminophen-induced hepatotoxicity [33]. Recent studies showed promising results for chronic hepatitis C virus patients using the antioxidant complex consisting of 94 mg silybin, 90 mg vitamin E, and 194 mg phospholipids (clinical trial phase III, No. NCT01935817). Another study (clinical trial phase IV No. NCT01002547) examining the use of PPARγ ligand and antioxidants in type 2 diabetes patients has received great attention. Our data indicated that all globins have stronger antioxidant capacities than glutathione or vitamin C. Together with the

reduced production of OH<sup>•</sup> and O<sub>2</sub><sup>•-</sup>, these findings demonstrate the safety and efficacy of globins for inhibiting collagen production and fibrosis development *in vitro* and *in vivo*, suggesting that globin proteins may represent promising antioxidant approaches for liver fibrosis and cirrhosis treatment in humans.

During the activation process, HSCs increase intracellular collagen production, resulting in the deposition of excess ECM protein in the extracellular space. Among ECM-degrading enzymes, MMP-1, an interstitial collagenase, plays an essential role in degrading collagen types I and III, which are major ECM components detected in liver fibrosis [34]. Under MB and NGB treatment, in parallel with the decreased detection of collagen type I in the medium, HHStECs induced the expression of MMP-1 at both the mRNA and protein levels (Fig. 5E). Increased MMP-1 levels could result from HHStEC deactivation by MB, NGB, or CYGB due to enhanced expression of ETS transcription factors that induce MMP-1 promoter activity [35].

The disulfide bond found in NGB and CYGB might be critical for their physiological functions by regulating the binding of exogenous ligands. The reduction of cysteine by incubation with dithiothreitol or the replacement of cysteine residues with alanine residues in NGB slowed the nitrite reduction rate [14]. In the present study, we observed that the loss of the disulfide bond in NGB led to decreased heme activity and superoxide-scavenging levels, and the attenuation of ROS-scavenging functions was related to the reduced capacity to suppress COL1A1 production. Replacement of the iron center of the heme group with cobalt ions in our previous study can reverse functions of CYGB on suppression of COL1A1, indicating the important role of heme moiety [17]. However, we did not observe the reduction in ROS-scavenging activity following His96 mutation in NGB, which may derive from compensatory activity of His64, a distal heme binding site. Previous studies suggested that His64 in NGB acts as an endogenous ligand [18], maintaining the bis-His conformation essential for neuroprotective NGB activity [36]. Further analysis targeting the regulatory contributions of these crucial Histidines to NGB functions in HSCs remains necessary.

In conclusion, our study revealed new applications for exogenous globin administration to treat liver fibrosis. MB and NGB as well as CYGB inhibited COL1A1 production by activated HSCs and prevented liver inflammation and liver fibrosis via intracellular ROS-scavenging functions. These results suggest that globins might provide a promising therapeutic option for advanced chronic fibrotic liver diseases.

### Grant support

V.N.H. was awarded the Japanese Government Scholarship for the Ph.D. course. This work was supported by the Grant-in-Aid for Scientific Research from the Japan Society for the Promotion of Science (JSPS Kaken C, 19K08428) and Gilead Science for Research Scholars Program in Liver Diseases (FY2019-2021) to L.T.T.T.; the Grant-in-Aid for Scientific Research from JSPS (19H03641), a Grant for Research Program on Hepatitis from the Japan Agency for Medical Research and Development (AMED-JP21fk0210050, JP21fk0210085, JP21fk0210058), and the Japan Agency for Medical Research and Development (AMED-CREST) Grant No: 21gm1010009h0004 to N.K..

### Author contributions

V.N.H. and L.T.T.T. provided the concept and design, data curation, and formal analysis; interpreted the data; conducted the experiments; drafted the manuscript; and obtained funding. N.Q.D., D.V.H., N.V.H., H.H., D.M.P., and T.H.H., conducted animal studies and experiments. H.S., Y.S., and D.O. provided materials and performed critical revision of the manuscript. M.S.-M. performed revision of the manuscript. K.Y., F.T., interpreted the data and performed critical revision of the manuscript for important intellectual content. N.K. contributed to the study concept and design, drafted the manuscript, performed critical revision of the manuscript for important intellectual content, funding acquisition, and

supervised the study. All authors had final approval of the submitted version.

### Declaration of competing interest

The authors declare no competing interests.

### Acknowledgments

We thank Drs. Kazuo Ikeda and Tsutomu Matsubara, and M.S. Yoshinori Okina for their helpful discussion. Quantitative RT-PCR analysis was performed at the Research Support Platform of Graduate School of Medicine, Osaka City University.

### Appendix A. Supplementary data

Supplementary data to this article can be found online at <https://doi.org/10.1016/j.redox.2022.102286>.

### References

- [1] E.L. Ellis, D.A. Mann, Clinical evidence for the regression of liver fibrosis, *J. Hepatol.* 56 (2012) 1171–1180.
- [2] S.L. Friedman, M. Pinzani, Hepatic fibrosis 2022: unmet needs and a blueprint for the future, *Hepatology* 75 (2022) 473–488.
- [3] Y.A. Lee, M.C. Wallace, S.L. Friedman, Pathobiology of liver fibrosis: a translational success story, *Gut* 64 (2015) 830–841.
- [4] P. Trivedi, S. Wang, S.L. Friedman, The power of plasticity-metabolic regulation of hepatic stellate cells, *Cell Metabol.* 33 (2021) 242–257.
- [5] T. Adachi, H. Togashi, A. Suzuki, S. Kasai, J. Ito, K. Sugahara, et al., NAD(P)H oxidase plays a crucial role in PDGF-induced proliferation of hepatic stellate cells, *Hepatology* 41 (2005) 1272–1281.
- [6] E.R. Garcia-Trevijano, M.J. Iriburu, L. Fontana, J.A. Dominguez-Rosales, A. Auster, A. Covarrubias-Pinedo, et al., Transforming growth factor beta1 induces the expression of alpha1(I) procollagen mRNA by a hydrogen peroxide-C/EBPbeta-dependent mechanism in rat hepatic stellate cells, *Hepatology* 29 (1999) 960–970.
- [7] J.X. Jiang, S. Venugopal, N. Serizawa, X. Chen, F. Scott, Y. Li, et al., Reduced nicotinamide adenine dinucleotide phosphate oxidase 2 plays a key role in stellate cell activation and liver fibrogenesis *in vivo*, *Gastroenterology* 139 (2010) 1375–1384.
- [8] A. Keppner, D. Maric, M. Correia, T.W. Koay, I.M.C. Orlando, S.N. Vinogradov, et al., Lessons from the post-genomic era: globin diversity beyond oxygen binding and transport, *Redox Biol* 37 (2020), 101687.
- [9] T. Burmester, B. Weich, S. Reinhardt, T. Hankeln, A vertebrate globin expressed in the brain, *Nature* 407 (2000) 520–523.
- [10] N. Kawada, D.B. Kristensen, K. Asahina, K. Nakatani, Y. Minamiyama, S. Seki, et al., Characterization of a stellate cell activation-associated protein (STAP) with peroxidase activity found in rat hepatic stellate cells, *J. Biol. Chem.* 276 (2001) 25318–25323.
- [11] A.J. Marengo-Rowe, Structure-function relations of human hemoglobins, *SAVE Proc.* 19 (2006) 239–245.
- [12] D. Hamdane, L. Kiger, S. Dewilde, B.N. Green, A. Pesce, J. Uzan, et al., The redox state of the cell regulates the ligand binding affinity of human neuroglobin and cytoglobin, *J. Biol. Chem.* 278 (2003) 51713–51721.
- [13] H. Tsujino, T. Yamashita, A. Nose, K. Kukino, H. Sawai, Y. Shiro, et al., Disulfide bonds regulate binding of exogenous ligand to human cytoglobin, *J. Inorg. Biochem.* 135 (2014) 20–27.
- [14] M. Tiso, J. Tejero, S. Basu, I. Azarov, X.D. Wang, V. Simplaceanu, et al., Human neuroglobin functions as a redox-regulated nitrite reductase, *J. Biol. Chem.* 286 (2011) 18277–18289.
- [15] T.T. Van Thuy, L.T. Thuy, K. Yoshizato, N. Kawada, Possible involvement of nitric oxide in enhanced liver injury and fibrogenesis during cholestasis in cytoglobin-deficient mice, *Sci. Rep.* 7 (2017), 41888.
- [16] N. Thi Thanh Hai, L.T.T. Thuy, A. Shiota, C. Kadono, A. Daikoku, D.V. Hoang, et al., Selective overexpression of cytoglobin in stellate cells attenuates thioacetamide-induced liver fibrosis in mice, *Sci. Rep.* 8 (2018), 17860.
- [17] N.Q. Dat, L.T.T. Thuy, V.N. Hieu, H. Hai, D.V. Hoang, N. Thi Thanh Hai, et al., Hexa histidine-tagged recombinant human cytoglobin deactivates hepatic stellate cells and inhibits liver fibrosis by scavenging reactive oxygen species, *Hepatology* 73 (2021) 2527–2545.
- [18] T. Uno, D. Ryu, H. Tsutsumi, Y. Tomisugi, Y. Ishikawa, A.J. Wilkinson, et al., Residues in the distal heme pocket of neuroglobin. Implications for the multiple ligand binding steps, *J. Biol. Chem.* 279 (2004) 5886–5893.
- [19] M. Bellei, C.A. Bortolotti, G. Di Rocco, M. Borsari, L. Lancellotti, A. Ranieri, et al., The influence of the Cys46/Cys55 disulfide bond on the redox and spectroscopic properties of human neuroglobin, *J. Inorg. Biochem.* 178 (2018) 70–86.
- [20] A. Braganza, K. Quesnelle, J. Bickta, C. Reyes, Y. Wang, M. Jessup, et al., Myoglobin induces mitochondrial fusion, thereby inhibiting breast cancer cell proliferation, *J. Biol. Chem.* 294 (2019) 7269–7282.

- [21] T.T. Thuy le, T. Morita, K. Yoshida, K. Wakasa, M. Iizuka, T. Ogawa, et al., Promotion of liver and lung tumorigenesis in DEN-treated cytoglobin-deficient mice, *Am. J. Pathol.* 179 (2011) 1050–1060.
- [22] S. Hanai, H. Tsujino, T. Yamashita, R. Torii, H. Sawai, Y. Shiro, et al., Roles of N- and C-terminal domains in the ligand-binding properties of cytoglobin, *J. Inorg. Biochem.* 179 (2018) 1–9.
- [23] A. Pesce, M. Bolognesi, A. Bocedi, P. Ascenzi, S. Dewilde, L. Moens, et al., Neuroglobin and cytoglobin. Fresh blood for the vertebrate globin family, *EMBO Rep* 3 (2002) 1146–1151.
- [24] B. Leader, Q.J. Baca, D.E. Golan, Protein therapeutics: a summary and pharmacological classification, *Nat. Rev. Drug Discov.* 7 (2008) 21–39.
- [25] P. Caraceni, M. Domenicali, A. Tovoli, L. Napoli, C.S. Ricci, M. Tufoni, et al., Clinical indications for the albumin use: still a controversial issue, *Eur. J. Intern. Med.* 24 (2013) 721–728.
- [26] H. Maeda, K. Hirata, H. Watanabe, Y. Ishima, V.T. Chuang, K. Taguchi, et al., Polythiol-containing, recombinant mannosylated-albumin is a superior CD68+/CD206+ Kupffer cell-targeted nanoantioxidant for treatment of two acute hepatitis models, *J. Pharmacol. Exp. Therapeut.* 352 (2015) 244–257.
- [27] H. Sakai, H. Horinouchi, E. Tsuchida, K. Kobayashi, Hemoglobin vesicles and red blood cells as carriers of carbon monoxide prior to oxygen for resuscitation after hemorrhagic shock in a rat model, *Shock* 31 (2009) 507–514.
- [28] H.-T. Schon, M. Bartneck, E. Borkham-Kamphorst, J. Nattermann, T. Lammers, F. Tacke, et al., Pharmacological intervention in hepatic stellate cell activation and hepatic fibrosis, *Front. Pharmacol.* 7 (2016), 33–33.
- [29] W.S. David, Myoglobinuria, *Neurol. Clin.* 18 (2000) 215–243.
- [30] J. Gburek, H. Birn, P.J. Verroust, B. Goj, C. Jacobsen, S.K. Moestrup, et al., Renal uptake of myoglobin is mediated by the endocytic receptors megalin and cubilin, *Am. J. Physiol. Ren. Physiol.* 285 (2003) F451–F458.
- [31] C.S. Lieber, S.J. Robins, J. Li, L.M. DeCarli, K.M. Mak, J.M. Fasulo, et al., Phosphatidylcholine protects against fibrosis and cirrhosis in the baboon, *Gastroenterology* 106 (1994) 152–159.
- [32] T. Toyama, H. Nakamura, Y. Harano, N. Yamauchi, A. Morita, T. Kirishima, et al., PPARalpha ligands activate antioxidant enzymes and suppress hepatic fibrosis in rats, *Biochem. Biophys. Res. Commun.* 324 (2004) 697–704.
- [33] K. Du, A. Farhood, H. Jaeschke, Mitochondria-targeted antioxidant Mito-Tempo protects against acetaminophen hepatotoxicity, *Arch. Toxicol.* 91 (2017) 761–773.
- [34] M.J.P. Arthur, Fibrogenesis - II. Metalloproteinases and their inhibitors in liver fibrosis, *Am. J. Physiol. Gastrointest. Liver Physiol.* 279 (2000) G245–G249.
- [35] J. Westermarck, A. Seth, V.M. Kahari, Differential regulation of interstitial collagenase (MMP-1) gene expression by ETS transcription factors, *Oncogene* 14 (1997) 2651–2660.
- [36] S. Watanabe, N. Takahashi, H. Uchida, K. Wakasugi, Human neuroglobin functions as an oxidative stress-responsive sensor for neuroprotection, *J. Biol. Chem.* 287 (2012) 30128–30138.